doi:10.1093/jmcb/mjv019
Published online March 17, 2015

Article

Fibroblast growth factor 7 is a nociceptive modulator secreted via large dense-core vesicles

Hui Liu[1], Qing-Feng Wu[1], Jia-Yin Li[1], Xing-Jun Liu[1], Kai-Cheng Li[1], Yan-Qing Zhong[1], Dan Wu[1], Qiong Wang[2], Yin-Jing Lu[1], Lan Bao[2,3], and Xu Zhang[1,3,*]

[1] Institute of Neuroscience and State Key Laboratory of Neuroscience, CAS Center for Excellence in Brain Science, Shanghai Institutes for Biological Sciences, Chinese Academy of Sciences, Shanghai 200031, China
[2] State Key Laboratory of Cell Biology, Institute of Biochemistry and Cell Biology, Shanghai Institutes for Biological Sciences, Chinese Academy of Sciences, Shanghai 200031, China
[3] School of Life Science and Technology, ShanghaiTech University, Shanghai 201210, China
* Correspondence to: Xu Zhang, E-mail: xu.zhang@ion.ac.cn

Fibroblast growth factor (FGF) 7, a member of FGF family, is initially found to be secreted from mesenchymal cells to repair epithelial tissues. However, its functions in the nervous system are largely unknown. The present study showed that FGF7 was a neuromodulator localized in the large dense-core vesicles (LDCVs) in nociceptive neurons. FGF7 was mainly expressed in small-diameter neurons of the dorsal root ganglion and could be transported to the dorsal spinal cord. Interestingly, FGF7 was mostly stored in LDCVs that did not contain neuropeptide substance P. Electrophysiological recordings in the spinal cord slice showed that buffer-applied FGF7 increased the amplitude of excitatory post-synaptic current evoked by stimulating the sensory afferent fibers. Behavior tests showed that intrathecally applied FGF7 potentiated the formalin-induced acute nociceptive response. Moreover, both acute and inflammatory nociceptive responses were significantly reduced in *Fgf7*-deficient mice. These results suggest that FGF7 exerts an excitatory modulation of nociceptive afferent transmission.

Keywords: fibroblast growth factor 7, dorsal root ganglion, large dense-core vesicle, nociceptive modulator, inflammatory pain

Introduction

Fibroblast growth factor (FGF) 7 is a member of FGF family, and its high affinity receptor is FGFR2b (Rubin et al., 1989; Miki et al., 1992). Previous studies suggest that FGF7 plays a role in the regulation of epithelial homeostasis in adult organs, particularly during epithelial protection and repair (Finch and Rubin, 2004). FGF7 has already been clinically used in the patients who suffer from oral mucositis resulting from cancer chemoradiotherapy (Spielberger et al., 2004). In the nervous system, FGF7 has been identified to act as target-derived presynaptic organizer in the hippocampal neurons (Terauchi et al., 2010). Our previous studies also found that the level of FGF7 mRNA (*Fgf7*) was upregulated in the dorsal root ganglion (DRG) neurons after peripheral nerve injury (Li et al., 2002; Xiao et al., 2002). However, the functions of FGF7 in the somatosensory circuits remain largely unknown.

In neurons, there are two secretory pathways, namely the constitutive secretory pathway for transport of growth factors and extracellular matrix proteins, and the regulated secretory pathway for transport of neurotransmitters and neuromodulators. Large dense-core vesicles (LDCVs) are major secretory vesicles of the regulated secretory pathway in neurons. Exocytosis of LDCVs is often triggered by extracellular stimulations that increase the intracellular Ca^{2+} level, leading to the release of their contents and the cell surface expression of the membrane proteins of LDCVs. In small DRG neurons, neuropeptides such as substance P and calcitonin gene-related peptide (CGRP) are packaged into LDCVs for Ca^{2+}-dependent secretion in response to noxious stimulations (Ma et al., 2008; Zhang et al., 2010; Gondre-Lewis et al., 2012). Moreover, many receptors, ion channels and other signaling molecules are associated with the membrane of LDCVs in small DRG neurons, enabling stimulus-induced membrane insertion (Wang et al., 2010; He et al., 2011; Zhao et al., 2011; Zhang et al., 2015). Under pathological conditions, altered secretion profile of LDCVs may contribute to the development of chronic pain (Zhang et al., 1998; Cahill et al., 2003; Hökfelt et al., 2003; Dolly and O'Connell, 2012). Analyzing the composition of these vesicles (Zhao et al., 2011) and studying the functions of LDCV contents are important for the understanding of nociceptive mechanisms. Although FGF7 is known as a secretory protein (Zhang et al., 2012), its subcellular localization and secretory pathway are unclear. Therefore, it was interesting to examine the subcellular distribution of FGF7 in the nociceptive neurons.

Received October 23, 2014. Revised January 27, 2015. Accepted February 2, 2015.

In the present study, we found the LDCV localization of FGF7 in small DRG neurons. FGF7 could enhance the excitatory synaptic transmission, and potentiate the formalin-induced nociceptive response. Moreover, FGF7 gene knockout (*Fgf7*$^{-/-}$) mice displayed defects in both acute and inflammatory nociceptive responses. These results suggest that FGF7 acts as an excitatory modulator in nociceptive afferent transmission.

Results

FGF7 expression in the sensory system

To study whether FGF7 had potential functions in the nervous system, we firstly examined the distribution pattern of *Fgf7* transcripts in mice using reverse transcription–polymerase chain reaction (RT–PCR). Total RNAs from DRG, dorsal spinal cord, and two brain regions, hippocampus and cerebellum, in which FGF7 mRNA has been detected previously (Umemori et al., 2004; Terauchi et al., 2010), were analyzed. We observed a relatively higher level of FGF7 mRNA in the DRG and cerebellum with real-time PCR (Figure 1A). Similar results were obtained using semi-quantitative PCR (Figure 1A). Then, by using *in situ* hybridization with the specific cRNA probe against *Fgf7*, we examined the cellular distribution of FGF7 mRNA in lumbar (L) 4 and L5 DRGs, and found that *Fgf7* was expressed in DRG neurons (Figure 1B). Analysis of cell-size distribution showed that most of these neurons were small DRG neurons, with a peak cross-section area from 300 to 500 μm^2 (Figure 1B). The hybridization signal in the neurons was specific, because the cytoplasmic *Fgf7* signal detected by antisense probe was not shown by the sense probe (Supplementary Figure S1A) and could be abolished by treatment with RNase A (Figure 1B).

Next, we used immunostaining to further localize FGF7 protein. We obtained three lines of evidence for the specificity of FGF7 antibody. First, COS-7 cells transfected with the plasmid expressing FGF7-myc could be immunostained with this antibody (Supplementary Figure S1B). Second, immunoblotting showed that the antibody recognized both the purified FGF7 and the exogenously expressed FGF7-myc (Supplementary Figure S1C). Thirdly, the immunostaining pattern in the DRG was abolished by the antibody pre-absorption with the corresponding antigen (Supplementary Figure S1D). Using this FGF7 antibody, we found that the FGF7 was mainly distributed in small DRG neurons (Figure 2A), consistent with the result of *in situ* hybridization. Small DRG neurons are often classified into the peptidergic subset and isolectin B4 (IB4)-positive (non-peptidergic) subset. FGF7 was distributed in both subsets, ~55% of FGF7-positive neurons contained neuropeptide CGRP (757/1377) and ~54%

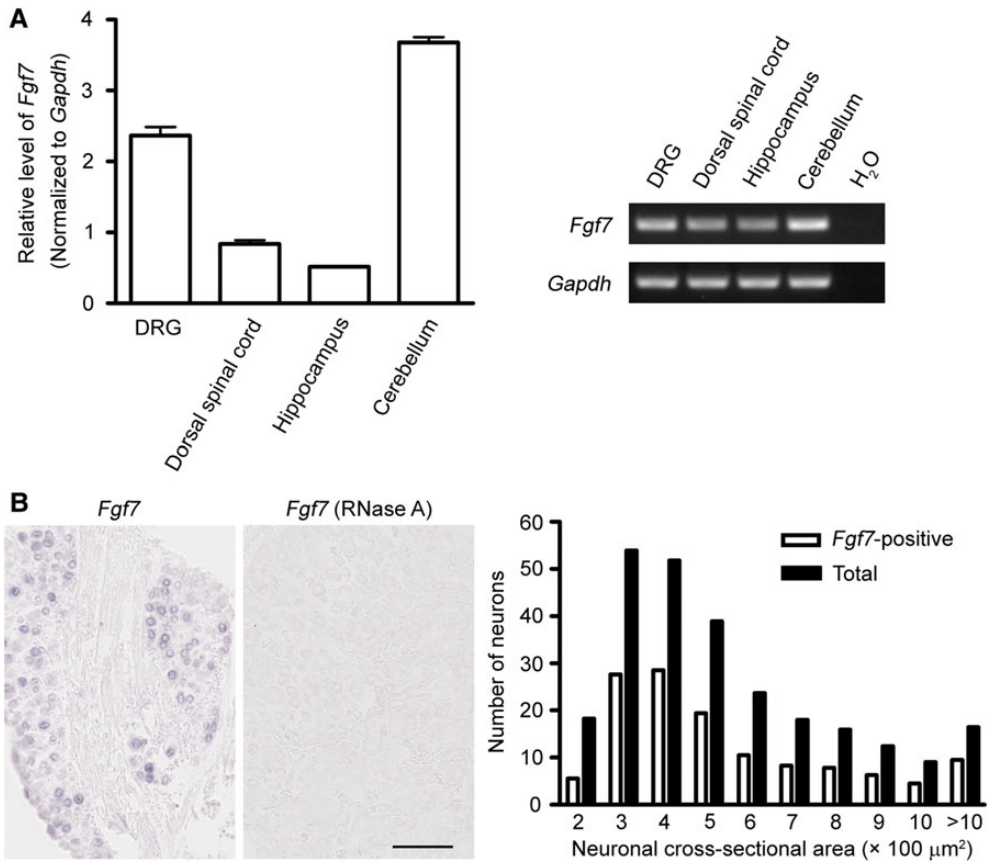

Figure 1 FGF7 mRNA is present in DRG neurons of mice. (**A**) Both real-time PCR (left) and semi-quantitative PCR (right) showed the presence of FGF7 mRNA in the DRG. *Gapdh* was used as control. (**B**) *In situ* hybridization showed that FGF7 mRNA was mainly present in small DRG neurons of mice. The hybridization signal in the section of DRG was abolished by the pretreatment with RNase A (100 mg/ml). The histogram showed the size distribution of *Fgf7*-positive neurons and total neurons. Scale bar, 100 μm.

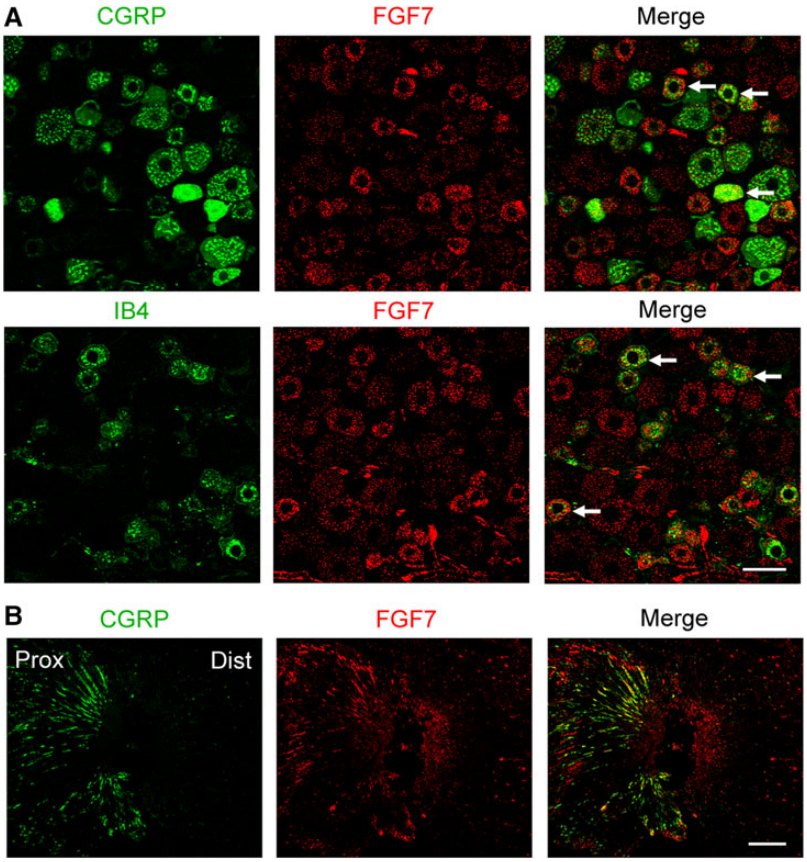

Figure 2 FGF7 protein is distributed in both the cell bodies and afferent fibers of DRG neurons. (**A**) Double-immunofluorescent staining showed that FGF7 was localized in both CGRP- and IB4-positive DRG neurons. Arrows indicate the examples of double-immunostained neurons. Scale bar, 50 μm. (**B**) One day after the dorsal root ligation, FGF7 was accumulated at the proximal (Prox) side, but not the distal (Dist) side, which was similar to CGRP. Scale bar, 200 μm.

of FGF7-positive neurons could be labeled by IB4 (953/1762) (Figure 2A).

The signaling of nociceptive stimuli is transmitted into the dorsal horn of spinal cord through thinly myelinated Aδ or unmyelinated C afferent fibers of small DRG neurons. To study the afferent transport of FGF7, we ligated L4 and L5 dorsal roots to block protein transport in the primary afferent fibers. FGF7 was accumulated in the nerve fibers in the proximal portion of the dorsal roots, similar to CGRP (Figure 2B), suggesting that FGF7 is transported to the central terminals in the dorsal spinal cord. However, we failed to detect any FGF7 staining in the afferent terminals in the dorsal horn of spinal cord. The expression and distribution pattern of FGF7 in the DRGs of mice were similar to that of rats (Supplementary Figure S2). Thus, the distribution of FGF7 suggests a potential role of FGF7 in somatosensation, especially in nociception.

Subcellular distribution of FGF7

We further examined the subcellular distribution of FGF7 in nociceptive afferent neurons. FGF7-immunoreactive vesicular structures were observed in the cytoplasma of small DRG neurons (Figure 3A). To further characterize the vesicular structure positive for FGF7, we used two-step sucrose-gradient centrifugation to separate different population of vesicles from the spinal dorsal horn of mice (Figure 3B). Chromogranin B (CGB) induces the biogenesis of LDCVs (Huh et al., 2003; Gondre-Lewis et al., 2012), and serves as a marker of LDCVs. We observed that FGF7 mainly appeared in the LDCV fractions labeled by CGB and CGRP (Figure 3B). Moreover, at the ultrastructural level, immunogold labeling of FGF7 was associated with LDCVs in the axonal terminals in the dorsal spinal cord (Figure 3C), consistent with the result of vesicular fraction analysis.

To further confirm the LDCV localization of FGF7, we co-transfected PC12 cells and cultured DRG neurons with the plasmids expressing FGF7-myc and CGB-green fluorescent protein (CGB-GFP). Double immunostaining with antibodies against myc, GFP, or FGF7 showed that FGF7 was largely localized at the CGB-positive vesicles (Figure 3D and E), indicating that FGF7 is indeed localized in LDCVs.

A recent study found that LDCVs in small DRG neurons could be classified into two distinct subsets, substance P-positive subsets containing CGRP and substance P-negative LDCVs containing β1 adrenergic receptor (AR) (Zhao et al., 2011). We found that 73.2% of FGF7-positive neurons contained β1 AR (1407/1921), whereas only 22.4% of FGF7-positive neurons contained substance P (347/1550) (Supplementary Figure S3). To further characterize FGF7-

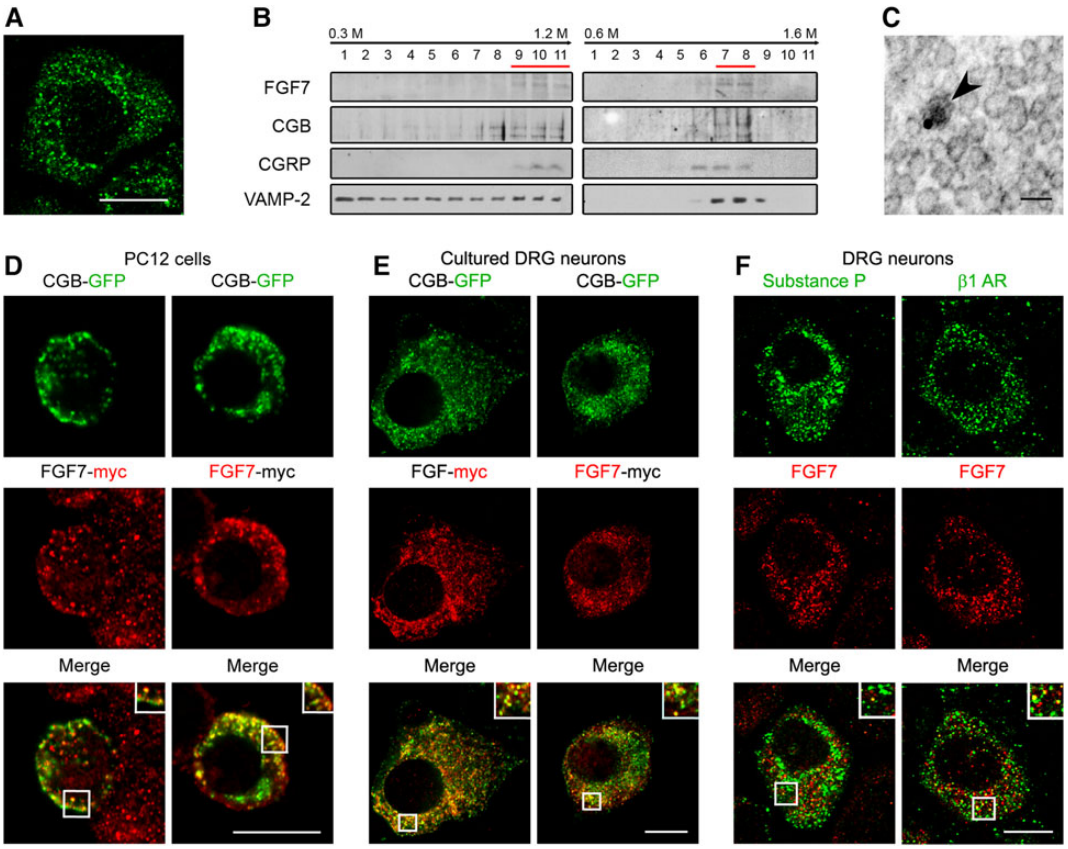

Figure 3 FGF7 is localized at the LDCVs in DRG neurons and PC12 cells. (**A**) Immunostaining with FGF7 antibody showed that FGF7 was localized in the vesicular structure of small DRG neurons. Scale bar, 10 μm. (**B**) Separation of different vesicles from the spinal dorsal horn of mice by two-step sucrose-gradient centrifugation. FGF7 was mainly distributed in CGB and CGRP-containing LDCV fractions (indicated by red lines). (**C**) Electromicrograph showed that immunogold labeling of FGF7 was associated with the LDCV (arrowhead) in the axonal terminal in the lamina II of spinal cord. Scale bar, 50 nm. (**D** and **E**) PC12 cells (**D**) and small DRG neurons cultured from the rat DRGs (**E**) were co-transfected with the plasmids expressing FGF7-myc and CGB-GFP. Double-immunofluorescent staining with antibodies against GFP and myc or FGF7 showed that FGF7 could be localized in CGB-positive LDCVs. Scale bar, 10 μm. (**F**) FGF7 was rarely found in substance P-positive LDCVs, but could be co-localized with β1 AR in some LDCVs. Scale bar, 10 μm. Insets in **D**, **E**, and **F** are high magnification of the area within white box.

positive vesicles, we analyzed neurons that were double-positive for FGF7 and substance P, or FGF7 and β1 AR. About 2.3% of FGF7-positive vesicles (40/1715, 17 neurons) were stained for substance P, while 13.8% of FGF7-positive vesicles (844/6131, 24 neurons) were labeled by β1 AR (Figure 3F). Taken together, both biochemical and cell biological evidence indicates the LDCV localization of FGF7 in nociceptive neurons, and the FGF7-containing LDCVs may represent an independent subpopulation of LDCVs in the neurons.

FGF7 facilitates nociceptive afferent neurotransmission

We then asked whether FGF7 could regulate the excitability of DRG neurons and afferent neurotransmission. The frequency of action potentials (AP) initiated by depolarizing ramp currents (0–200 pA, 1s) was unaffected by FGF7 treatment in dissociated DRG neurons (Figure 4A). To further examine the effect of FGF7 treatment on the synaptic transmission between primary afferent terminals and spinal cord neurons, we used the whole-cell recording of the dorsal root-attached spinal cord slices to analyze the excitatory postsynaptic currents (EPSC) of the interneurons in the spinal lamina II, which is a translucent band in the superficial dorsal horn of spinal cord slice under the microscope. FGF7 treatment did not significantly affect the frequency or the amplitude of spontaneous EPSC (sEPSC) (Figure 4B). However, the buffer-applied FGF7 increased the amplitude of evoked EPSC (eEPSC) that was triggered by electrically stimulating the afferent fibers in the dorsal root at 0.2 Hz (Figure 4C), indicating that FGF7 facilitates the excitatory synaptic transmission at the axon terminals in an activity-dependent manner.

Subcutaneous injection with formalin into the hindpaw could induce acute nociceptive responses in both rats (flinching behavior response) and mice (licking behavior response) (Dubuisson and Dennis, 1977). We found that intrathecally (i.t.) applied FGF7 facilitated the acute nociceptive response induced by formalin in rats (Figure 4D), whereas the formalin-induced response could be alleviated by intrathecal injection with the antibody against FGF7 to neutralize the endogenous FGF7 (Figure 4E). These results of behavior tests were correlated with the effect of FGF7 on the afferent synaptic transmission, suggesting that FGF7 facilitates the nociceptive response.

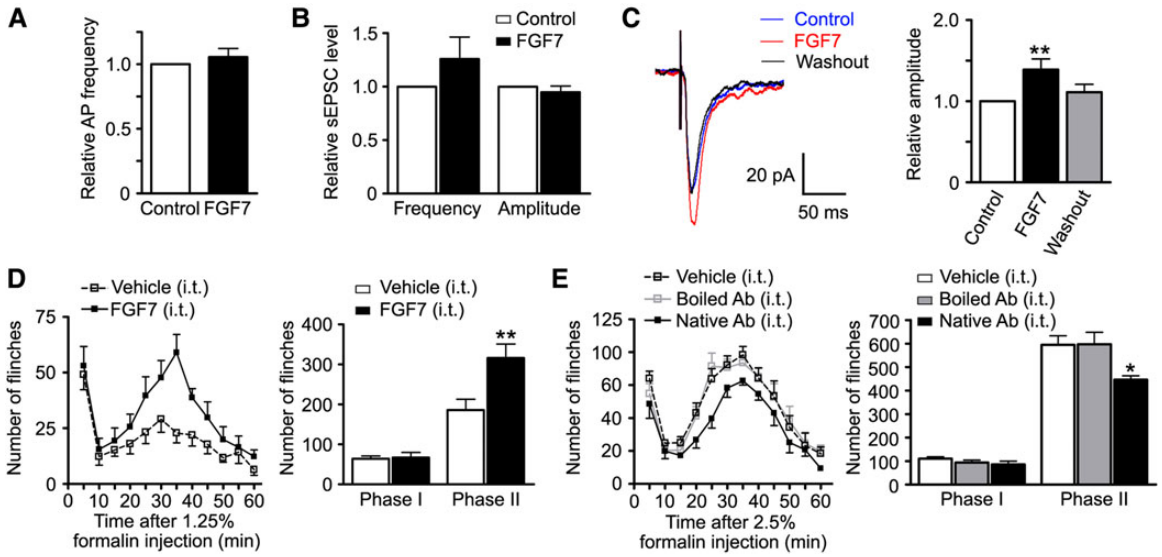

Figure 4 FGF7 enhances the afferent synaptic transmission and formalin-induced nociceptive response. (**A**) Whole-cell patch-clamp recording showed that FGF7 treatment (100 ng/ml) did not affect the frequency of APs triggered by current injection in small neurons ($n = 10$) dissociated from rat DRGs. (**B**) Whole-cell recording in the lamina II neurons ($n = 11$) in spinal cord slices of rats showed that sEPSCs were not significantly changed by FGF7 treatment (100 ng/ml). (**C**) The recording traces showed that the amplitude of eEPSC induced by stimulating the dorsal root at 0.2 Hz was increased after treatment with FGF7 (100 ng/ml) and returned to the basal level after washout. The histogram showed the statistical analysis of the data ($n = 8$ neurons among 14 recorded ones). (**D** and **E**) In the formalin test of rats, 0–10 min was considered to be phase I and 10–50 min was phase II. Intrathecal treatment with FGF7 (0.5 μg, $n = 11$ for both groups) enhanced the nociceptive response ($P < 0.001$, two-way ANOVA between vehicle and FGF7 treatment) with more nociceptive responses in the phase II, whereas native FGF7 antibody (Ab, 1 μg, $n = 10$ for vehicle, $n = 11$ for boiled Ab, $n = 8$ for native Ab) reduced the response ($P < 0.001$, two-way ANOVA between boiled and native Ab) with less nociceptive responses in the phase II. *$P < 0.05$ and **$P < 0.01$ versus control for FGF7 treatment or boiled Ab for FGF7 antibody treatment. Error bars indicate SEM.

Furthermore, we designed specific primers against *Fgfr2b* and found that FGFR2b mRNA could be detected in the dorsal spinal cord of mice, with a relatively lower level in the DRG (Supplementary Figure S4A). However, intrathecal treatment with FGF7 did not change basal thermal threshold of rats (Supplementary Figure S4B), consistent with the notion that FGF7 effect is activity-dependent. We also performed formalin test after intraplantar (i.p.l.) injection with FGF7 and found that formalin-induced behavior response of rats was not affected by the peripheral treatment (Supplementary Figure S4C), suggesting that FGF7 regulates nociceptive responses at the spinal cord level.

Fgf7-deficient mice display defects in both acute and inflammatory nociceptive responses

Then, the FGF7 function was confirmed by using the $Fgf7^{-/-}$ mouse in which FGF7 is truncated and loses functions (Ron et al., 1993). We indeed found that the mRNA encoding the signal peptide and at least 70 amino acids in the N-terminus of FGF7 was absent, while the 3′ region of FGF7 mRNA still existed (Supplementary Figure S5C). Previous studies showed that the development of $Fgf7^{-/-}$ mice was basically normal (Guo et al., 1996). We examined the morphology of the DRG and spinal cord of mutant mice, as well as the expression of various molecular markers of DRG neurons and their distribution in the afferent fibers in the dorsal horn of spinal cord. There were no marked differences between wild-type ($Fgf7^{+/+}$) and $Fgf7^{-/-}$ mice (Supplementary Figure S6). $Fgf7^{-/-}$ mice also showed normal performances in the accelerating rotarod test and the open field test, indicating their normal motor functions (Supplementary Figure S5D and E).

We next asked whether the deficiency of *Fgf7* could influence the nociceptive behavior. We firstly used thermal and mechanical stimuli to test acute nociceptive thresholds of $Fgf7^{-/-}$ mice. Although there were no differences between $Fgf7^{-/-}$ and $Fgf7^{+/+}$ mice in hot plate and von Frey test (Supplementary Figure S5F and G), $Fgf7^{-/-}$ mice displayed longer latency in tail flick assay at 52°C (Figure 5A), which mainly represents the spinal reaction to the noxious heat. Thus, FGF7 may regulate the baseline of thermal nociceptive responses. We also found that the phase II of formalin-induced response was significantly reduced in *Fgf7*-deficient mice (Figure 5B). Furthermore, Complete Freund's Adjuvant (CFA)-induced thermal hyperalgesia and mechanical allodynia were significantly alleviated in $Fgf7^{-/-}$ mice compared with $Fgf7^{+/+}$ mice (Figure 5C and D). We noticed that the extent of difference between $Fgf7^{+/+}$ and $Fgf7^{-/-}$ mice was kept similar before and during the inflammation, suggesting the association between FGF7 effects on the baseline of thermal nociception and the inflammation-induced thermal hyperalgesia. These results suggest that both acute and persistent inflammatory pain is enhanced by FGF7 expressed in the nociceptive afferent neurons.

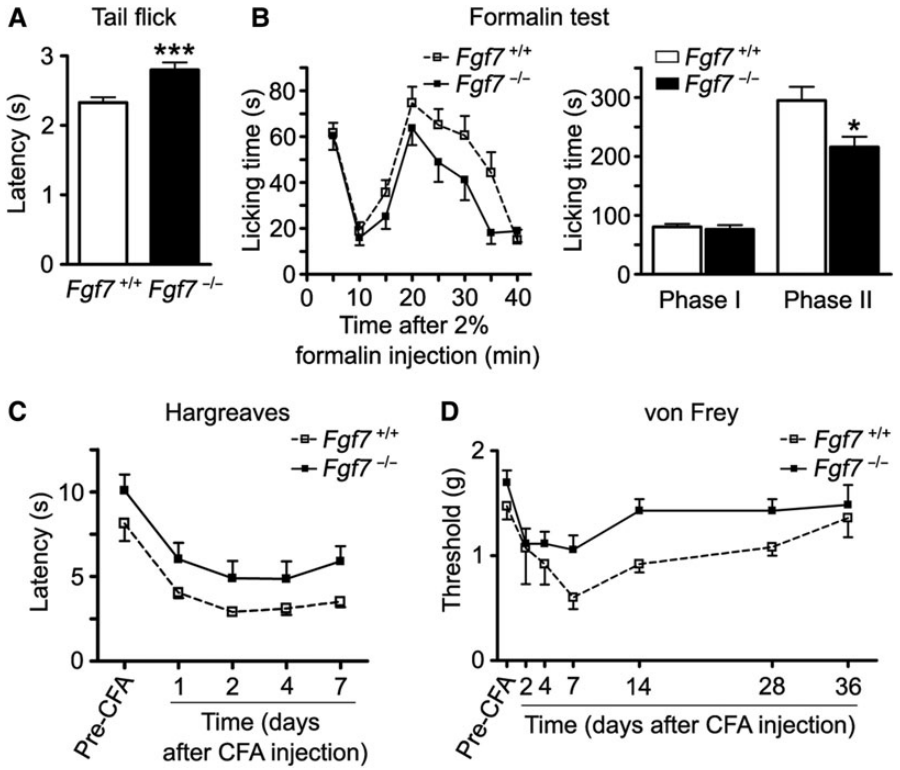

Figure 5 Formalin- and CFA-induced nociceptive responses are reduced in *Fgf7*$^{-/-}$ mice. (**A**) Tail flick test showed that the thermal latency of *Fgf7*$^{-/-}$ mice at 52°C was longer than that of *Fgf7*$^{+/+}$ mice ($n = 26$ for *Fgf7*$^{+/+}$ and $n = 18$ for *Fgf7*$^{-/-}$). (**B**) The formalin-induced response was significantly reduced in *Fgf7*$^{-/-}$ mice (2% formalin; $n = 21$ for *Fgf7*$^{+/+}$ and $n = 15$ for *Fgf7*$^{-/-}$; $P < 0.01$, two-way ANOVA between *Fgf7*$^{+/+}$ and *Fgf7*$^{-/-}$ mice) with less nociceptive responses in the phase II (phase I: 0–10 min, phase II: 10–40 min). (**C** and **D**) The CFA-induced thermal hyperalgesia ($n = 5$ for both *Fgf7*$^{+/+}$ and *Fgf7*$^{-/-}$) (**C**) and mechanical allodynia ($n = 5$ for *Fgf7*$^{+/+}$ and $n = 7$ for *Fgf7*$^{-/-}$) (**D**) were significantly alleviated in *Fgf7*$^{-/-}$ mice ($P < 0.05$, two-way ANOVA between *Fgf7*$^{+/+}$ and *Fgf7*$^{-/-}$ mice). Pre-CFA indicates the basal threshold before CFA injection. *$P < 0.05$ and ***$P < 0.001$ versus *Fgf7*$^{-/-}$ mice. Error bars indicate SEM.

Discussion

The present study reveals that FGF7 synthesized in nociceptive afferent neurons is transported mainly via LDCVs to the central terminals. This could be a cellular mechanism for FGF7 to facilitate the excitatory afferent transmission and enhance both acute and persistent nociceptive responses. Thus, FGF7 is an excitatory modulator in the spinal nociceptive circuit.

Our previous study showed the existence of FGF7 mRNA in rat DRG neurons and upregulation of FGF7 expression after peripheral nerve injury (Li et al., 2002; Xiao et al., 2002). This finding has been confirmed by recent RNA sequencing study (Perkins et al., 2014). In the present study, FGF7 mRNA was also detected in the mouse DRGs by real-time PCR. Furthermore, *in situ* hybridization showed that *Fgf7* was mainly expressed in small DRG neurons. However, the Allen brain atlas could not detect FGF7 mRNA in the DRGs of P4 mice (http://mousespinal.brain-map.org/imageseries/show.html?id=100003765). Therefore, more detailed analysis with careful probe design and proper experimental conditions are required for detecting individual genes in the tissue, although the large-scale detection may provide a global view of gene expression. We found a relatively high level of FGF7 mRNA in the DRG and cerebellum, consistent with previous reports showing the expression of FGF7 in the hippocampus and cerebellum (Umemori et al., 2004; Terauchi et al., 2010).

Since the presence of substance P in small DRG neurons was reported, the expression, localization, and function of many neuropeptides and secretory proteins in these neurons under normal and pathological pain conditions were extensively studied (Hökfelt et al., 1994; Salio et al., 2005). Following peripheral inflammation or nerve injury, changes in the expression profile of neuropeptides and secretory proteins in primary afferent neurons may contribute to the development of chronic pain (Hökfelt et al., 2003; Lin et al., 2011; Dolly and O'Connell, 2012). In the present study, both biochemical and morphological evidence showed the LDCV localization of FGF7 in small DRG neurons. Particularly, the LDCV localization of FGF7 was proved by co-localization of the LDCV marker, CGB (Huh et al., 2003; Gondre-Lewis et al., 2012), with the exogenously expressed FGF7 in the LDCVs of transfected PC12 cells and cultured DRG neurons. Previous study reported the existence of different subpopulations of LDCVs with distinct cargoes in small DRG neurons, such as β2 AR in the substance P-positive LDCVs and β1 AR in the substance P-negative LDCVs (Zhao et al., 2011), suggesting the differential functions of LDCVs. However, the secretory substances in the substance

P-negative LDCVs have not been identified. The present finding of FGF7 in the substance P-negative LDCVs provides the first evidence for the secretory contents in that subpopulation of LDCVs.

In this study, we also found that although ~73% of FGF7-positive DRG neurons contained β1 AR, only ~14% of FGF7-containing LDCVs were β1 AR-positive. Co-localization of β1 AR and FGF7 in a fraction of LDCVs suggests that the release of FGF7 and the plasma membrane insertion of β1 AR could be coupled when the exocytosis of these LDCVs occurs. The deregulation of β-adrenergic activity could result in chronic pain, and the intradermal treatment with epinephrine, the endogenous ligand for β-ARs, could induce pain hypersensitivity (Coderre et al., 1990; Khasar et al., 1999). Previous studies mainly focused on the roles of β2 AR and β3 AR in the nociceptive neurotransmission (Hartung et al., 2014). The functions of β1 AR remain to be investigated. Co-localization of β1 AR in some FGF7-containing LDCVs suggests that peripheral stimulations could induce FGF7 release and regulate the adrenergic signaling through the coupled membrane insertion of β1 AR.

Previous studies showed changes in the expression of growth-associated factors after nerve injury (Ji et al., 1995; Li et al., 2002; Xiao et al., 2002; Lin et al., 2011) and their roles in the development of neuropathic pain (Coull et al., 2005; Madiai et al., 2005; Yamanaka et al., 2007; Furusho et al., 2009). The present study showed that FGF7 was expressed in small DRG neurons and modulated both acute and inflammatory nociceptive responses. Although we failed to immunostain FGF7 in the afferent terminals in the dorsal horn of spinal cord, the accumulation of FGF7 in the ligated dorsal root indicates that FGF7 could be transported to the central axon terminals. A high level of *Fgfr2b* was present in the dorsal horn of spinal cord, suggesting that FGF7 released from the afferent terminals could act at the local cells. It is also possible that FGF7 presynaptically regulates neurotransmission, since a relatively low level of *Fgfr2b* was found in the DRG. However, the specific antibody against FGFR2b is not available. Therefore, the cellular localization of FGF7 receptors in the DRG and spinal cord remains to be studied.

Behavior tests showed that the basal level of thermal nociceptive response and the inflammation-induced thermal and mechanical nociceptive hypersensitivity were partially reduced in *Fgf7*-deficient mice, suggesting an important role of the endogenous FGF7 in the regulatory mechanism of pain. Tail flick test and Hargreaves test often refer to the spinal responses to noxious thermal stimuli. The results of both tail flick test and Hargreaves test showed the effect of FGF7 on the basal level of thermal response, suggesting the spinal function of FGF7. Hot plate test represents the functions mediated mainly by the supraspinal regulatory system. Together with the results of tail flick test and Hargreaves test in *Fgf7*-deficient mice, the negative result of hot plate test also supports that FGF7 mainly acts at the spinal cord level. Such an effect of FGF7 could be associated with the inflammation-induced thermal hyperalgesia. The regulatory mechanism of FGF7 in the inflammation-induced mechanical nociceptive hypersensitivity remains to be further investigated.

We conclude that FGF7 is expressed in sensory afferent neurons and localized in a unique subpopulation of LDCVs. FGF7 functions as a neuromodulator to facilitate the excitatory afferent neurotransmission, and enhance both acute and inflammatory nociceptive responses. Thus, FGF7 is an excitatory modulator released from nociceptive afferent neurons via LDCVs. Inhibition of the FGF7 signaling in the nociceptive circuit may contribute to a potential strategy for inflammatory pain therapy.

Materials and methods

Animals

All experiments were approved by the Committee of Use of Laboratory Animals and Common Facility, Institute of Neuroscience, Chinese Academy of Sciences. Male Sprague Dawley (SD) rats and C57BL/6 mice were provided by Shanghai Laboratory Animal Center (Shanghai, China) and housed under a 12-h light/dark cycle at 22°C–26°C. *Fgf7*$^{-/-}$ mice were purchased from the Jackson Laboratory and generated as previously described (Guo et al., 1996). Briefly, a targeting vector containing a neomycin-resistant gene was used to disrupt the exon 2 region of *Fgf7* gene (Supplementary Figure S5A). The genotyping primers are listed in Supplementary Table S1.

RT–PCR

Total RNAs (2 μg) from various tissues were reverse transcribed with SuperScript II reverse transcriptase (Invitrogen). Primers for mouse *Fgf7*, *Fgfr2b*, and *Glyceraldehyde-3-phosphate dehydrogenase* (*Gapdh*) genes (Supplementary Table S1) were used to perform real-time PCR experiments with SYBR Premix Ex Taq II Kit (Takara). The mRNA level of *Fgf7* and *Fgfr2b* were normalized to *Gapdh*. Primers for the 5′ and 3′ region of mouse *Fgf7* and *Gapdh* (Supplementary Table S1) were used to perform semi-quantitative PCR with Ex Taq DNA Polymerase Kit (Takara). The PCR products were separated on 1.2% agarose gels and photographed under UV illumination.

In situ hybridization

The experiment was performed according to our previous protocol (Wang et al., 2010). DNA fragments were amplified with PCR primers (Supplementary Table S1) for mouse *Fgf7* (NM_008008) and incorporated into pGEM-T easy vector. Then the fragment was amplified with T7/SP6 primers and transcribed into the digoxigenin-labeled cRNA probe using SP6 (antisense) and T7 (sense) RNA polymerase (Roche). Tissue sections pretreated with or without RNase A (100 mg/ml) were used for both antisense and sense probes (Wilcox, 1993). Specific signals with the antisense probe were located in the cytoplasm, which was absent with the sense probe and could be abolished by RNase A treatment (Figure 1B and Supplementary Figure S1A). The nonspecific signal in the nucleus generated by the sense probe could not be abolished by RNase A pretreatment (Supplementary Figure S1A). To determine the size distribution of neurons, the neuron profiles with a clear nucleus were selected and the data were pooled from three mice.

Cell culture and transfection

PC12 cells were cultured in DMEM (GIBCO) containing 10% horse serum and 5% fetal bovine serum. COS-7 and HEK293T cells were

cultured in DMEM (GIBCO) containing 10% fetal bovine serum. These cells were transfected with plasmids by 10 μl lipofectamine 2000 (Invitrogen) according to the manufacturer's protocol (35-mm dish) and cultured in medium containing serum for 2 days.

Immunohistochemistry/immunocytochemistry

Adult male rats and mice were fixed with 4% paraformaldehyde. Cryostat sections of L4 and L5 DRGs and spinal cord segments were stained with primary antibodies against FGF7 (1:400, R&D Systems), peripherin (1:2000, Chemicon), NF200 (1:2000, Sigma), PKC-γ (1:500, Santa Cruz), or NeuN (1:500, Chemicon), or with CGRP (1:1000, Dia Sorin and AbD Serotec), substance P (1:500, Neuromics), or β1-AR (1:400, Santa Cruz), and followed by secondary antibodies conjugated with FITC or/and Cy3 (1:100, Jackson laboratory), or 10 μg/ml fluorescein-conjugated IB4 (Vector Laboratories). Images from at least four rats were used to analyze the distribution pattern of FGF7.

Cultured DRG neurons and PC12 cells co-transfected with the plasmids expressing FGF7-myc and CGB-GFP were fixed with 4% paraformaldehyde. These cells were stained with primary antibodies against GFP (1:500, Roche) and myc (1:500, Sigma) or FGF7 (1:400, R&D Systems), and followed by secondary antibodies conjugated with FITC and Cy3, respectively. Images from the DRGs of four rats were used to analyze the vesicle distribution pattern of FGF7. Cultured COS-7 and HEK293T cells transfected with the plasmids expressing FGF7-myc were fixed and stained with primary antibodies against myc (1:500, Sigma) and FGF7 (1:400, R&D Systems) or FGF7 alone (1:200, Santa Cruz), and followed by secondary antibodies conjugated with FITC and Cy3, respectively. Specificity of FGF7 immunostaining was tested by detection of the exogenously expressed FGF7 and pre-absorption of antibodies with 1×10^{-6} M corresponding immunogens (Supplementary Figure S1B, D, and E).

Subcellular fractionation

The experiment was performed according to our previous protocol (Zhao et al., 2011). Two continuous sucrose gradients ranged from 0.3 to 1.2 M and 0.6 to 1.6 M sucrose/4 mM HEPES (pH 7.4) were used to separate different subcellular fractions from the spinal dorsal horn of mice. Samples were analyzed by immunoblotting with antibodies against FGF7 (1:500, R&D Systems), CGB (1:500, Santa Cruz), CGRP (1:1000, Dia Sorin), or vesicle-associated membrane protein 2 (VAMP-2; 1:2000, Synaptic Systems) to examine the subcellular distribution profile of FGF7. Specificity of FGF7 immunoblotting was tested by detection of the purified FGF7 and the exogenously expressed FGF7 (Supplementary Figure S1C).

Electron microscopy

Spinal cord sections from adult mice were processed for post-embedding immunogold staining according to our previous protocol (Zhao et al., 2011). Briefly, mice were fixed with 4% paraformaldehyde containing 0.1% picric acid and 0.05% glutaraldehyde. After post-fixation, L4 and L5 spinal cord was cut into 200-μm slices, passed through 0.5% osmic oxide for 30 min, dehydrated, embedded in Epon 812, and polymerized. The ultrathin sections of the superficial dorsal horn were stained with antibodies against FGF7 (1:100, Santa Cruz), and then with immunogold (15 nm). Specificity of this FGF7 antibody was tested by detecting the exogenously expressed FGF7 (Supplementary Figure S1E).

Electrophysiological recording

L4 and L5 DRG neurons of SD rats were acutely dissociated, digested, and incubated in normal extracellular solution (ECS) containing 150 mM NaCl, 5 mM KCl, 2.5 mM $CaCl_2$, 1 mM $MgCl_2$, 10 mM HEPES, and 10 mM glucose (pH 7.4). Whole-cell recordings were performed on small DRG neurons (<30 μm) within 12 h after plating. The pipette solution contained 153 mM KCl, 1 mM $MgCl_2$, 10 mM NaCl, 10 mM HEPES, and 4 mM Na-ATP (pH 7.2). Depolarizing currents were injected to the neuron to induce APs before or after treatment with recombinant mouse FGF7 (100 ng/ml; R&D Systems) for 5 min and washout. Data were collected with an EPC-9 patch-clamp amplifier and the Pulse software (version 8.31; HEKA Elektronik).

Spinal cord slice (400 μm in thickness) with or without an attached dorsal root was made and perfused in oxygen-bubbled Kreb's solution to perform blind whole-cell recording (Nakatsuka et al., 1999; Li et al., 2011). The composition of the pipette solution was 135 mM K-gluconate, 0.5 mM $CaCl_2$, 2 mM $MgCl_2$, 5 mM KCl, 5 mM EGTA, 5 mM HEPES, and 5 mM glucose (all from Sigma). Spontaneous EPSC or eEPSC was recorded by Axopatch 200B (Molecular Devices), and analyzed using pCLAMP10.1 (Molecular Devices). The stimuli generated by a constant-current stimulator (Electronic Stimulator; Nihon Kohden) were delivered to the dorsal root through a suction electrode to sufficiently recruit Aδ- and C-fibers. The responses were considered as monosynaptic in origin when the latency remained constant and no failure during stimulation at 20 Hz for the eEPSCs of Aδ-fiber and at 2 Hz for the eEPSCs of C-fiber (Yoshimura and Nishi, 1993; Ataka et al., 2000; Luo et al., 2002; Lao et al., 2004; Li et al., 2011). The eEPSC was recorded by stimulating the dorsal root at 0.2 Hz based on previous studies (Nakatsuka et al., 1999; Ataka et al., 2000; Luo et al., 2002; Lao et al., 2004; Li et al., 2011). The recorded neuron was stable in six repeats of stimulation and lasted for at least 20 min when the FGF7 treatment and washout were performed.

Behavior tests

All behavior tests were carried out blindly and followed the guidelines of the International Association for the Study of Pain. For the formalin test in adult (2 months) male SD rats, intrathecal treatment with various drugs was done as previously described (Liu et al., 2012). FGF7 antibody that was boiled for 10 min at 100°C was used as the negative control for the treatment of native FGF7 antibody. Formalin (50 μl, 1.25% for FGF7 treatment or 2.5% for FGF7 antibody treatment; Sigma) was injected subcutaneously into the dorsal surface of the left hindpaw with a 30 gauge needle at 0.5 h after drug treatment. The rats were placed into the chambers and their nociceptive responses were video-recorded for 1 h immediately after formalin injection. The number of flinch response was counted during each 5-min interval for each rat. To measure the basal thermal threshold of rats, the duration from the onset of heat stimuli with a radiant heat stimulator

(BME-410C; CAMS) to the occurrence of a hindpaw withdrawal reflex, with a cutoff time of 20 sec, was calculated as the latency.

Behavior tests of adult *Fgf7*$^{+/+}$ and *Fgf7*$^{-/-}$ mice (2.5–3 months for both male and female) were performed as previously described (Li et al., 2011). Each mouse was tested for baseline heat latency by immersing one-third of its tail in 52°C water or placing them on the hot plate of 50°C, 52°C, or 55°C and recording the time to response. Formalin (20 μl, 2%) was injected into the plantar surface of the left hindpaw to test their tonic nociceptive responses to chemical stimuli. The licking and lifting time of the injected hindpaw during each 5-min interval for 40 min was counted. Mechanical or thermal threshold was determined by using von Frey filaments or the radiant heat stimulator (Hargreaves Apparatus; Ugo Basile). For the von Frey test, we used filaments with incremental stiffness (0.16, 0.4, 0.6, 1.0, 1.4, 2.0, and 4.0 g). The hindpaw was perpendicularly touched by a filament to cause slight buckling (5 sec) and tested for five times (5-min interval). The withdrawal of the paw was recognized as a positive response. The mechanical threshold of a mouse was the minimal stiffness of the filament that induced the paw withdrawal with $>50\%$ occurrence frequency. Mice were also tested with the accelerating rotarod (4–40 rpm) and the open field test (total movement distance in 5 min).

The relative long-term behavior tests for the inflammation model with CFA were carried out only for male *Fgf7*$^{+/+}$ and *Fgf7*$^{-/-}$ mice to avoid the estrogen influence. After testing the baseline threshold, CFA (20 μl) was injected into the hindpaw to produce the inflammation model and the threshold was further tested for each mouse as before.

Statistical analysis

Image-Pro Plus 5.0 software (Media Cybernetics, Silver Spring) was used to analyze the images. Comparisons between two groups were performed by unpaired or paired Student's *t*-test. Comparisons among multiple groups were performed using two-way ANOVA with a *post hoc* Bonferroni's test. Data are presented as mean ± SEM. Differences were considered to reach statistical significance when $P < 0.05$.

Supplementary material

Supplementary material is available at *Journal of Molecular Cell Biology* online.

Funding

This work was supported by the National Natural Science Foundation of China (31130066) and the Strategic Priority Research Program (B) of Chinese Academy of Sciences (XDB01020300).

Conflict of interest: none declared.

References

Ataka, T., Kumamoto, E., Shimoji, K., et al. (2000). Baclofen inhibits more effectively C-afferent than Aδ-afferent glutamatergic transmission in substantia gelatinosa neurons of adult rat spinal cord slices. Pain *86*, 273–282.

Cahill, C.M., Morinville, A., Hoffert, C., et al. (2003). Up-regulation and trafficking of δ opioid receptor in a model of chronic inflammation: implications for pain control. Pain *101*, 199–208.

Coderre, T.J., Basbaum, A.I., Dallman, M.F., et al. (1990). Epinephrine exacerbates arthritis by an action at presynaptic B_2-adrenoceptors. Neuroscience *34*, 521–523.

Coull, J.A., Beggs, S., Boudreau, D., et al. (2005). BDNF from microglia causes the shift in neuronal anion gradient underlying neuropathic pain. Nature *438*, 1017–1021.

Dolly, J.O., and O'Connell, M.A. (2012). Neurotherapeutics to inhibit exocytosis from sensory neurons for the control of chronic pain. Curr. Opin. Pharmacol. *12*, 100–108.

Dubuisson, D., and Dennis, S.G. (1977). The formalin test: a quantitative study of the analgesic effects of morphine, meperidine, and brain stem stimulation in rats and cats. Pain *4*, 161–174.

Finch, P.W., and Rubin, J.S. (2004). Keratinocyte growth factor/fibroblast growth factor 7, a homeostatic factor with therapeutic potential for epithelial protection and repair. Adv. Cancer Res. *91*, 69–136.

Furusho, M., Dupree, J.L., Bryant, M., et al. (2009). Disruption of fibroblast growth factor receptor signaling in nonmyelinating Schwann cells causes sensory axonal neuropathy and impairment of thermal pain sensitivity. J. Neurosci. *29*, 1608–1614.

Gondre-Lewis, M.C., Park, J.J., and Loh, Y.P. (2012). Cellular mechanisms for the biogenesis and transport of synaptic and dense-core vesicles. Int. Rev. Cell Mol. Biol. *299*, 27–115.

Guo, L., Degenstein, L., and Fuchs, E. (1996). Keratinocyte growth factor is required for hair development but not for wound healing. Genes Dev. *10*, 165–175.

Hartung, J.E., Ciszek, B.P., and Nackley, A.G. (2014). β_2- and β_3-adrenergic receptors drive COMT-dependent pain by increasing production of nitric oxide and cytokines. Pain *155*, 1346–1355.

He, S.Q., Zhang, Z.N., Guan, J.S., et al. (2011). Facilitation of μ-opioid receptor activity by preventing δ-opioid receptor-mediated codegradation. Neuron *69*, 120–131.

Hökfelt, T., Zhang, X., and Wiesenfeld-Hallin, Z. (1994). Messenger plasticity in primary sensory neurons following axotomy and its functional implications. Trends Neurosci. *17*, 22–30.

Hökfelt, T., Bartfai, T., and Bloom, F. (2003). Neuropeptides: opportunities for drug discovery. Lancet Neurol. *2*, 463–472.

Huh, Y.H., Jeon, S.H., and Yoo, S.H. (2003). Chromogranin B-induced secretory granule biogenesis: comparison with the similar role of chromogranin A. J. Biol. Chem. *278*, 40581–40589.

Ji, R.R., Zhang, Q., Zhang, X., et al. (1995). Prominent expression of bFGF in dorsal root ganglia after axotomy. Eur. J. Neurosci. *7*, 2458–2468.

Khasar, S.G., McCarter, G., and Levine, J.D. (1999). Epinephrine produces a β-adrenergic receptor-mediated mechanical hyperalgesia and in vitro sensitization of rat nociceptors. J. Neurophysiol. *81*, 1104–1112.

Lao, L.J., Kawasaki, Y., Yang, K., et al. (2004). Modulation by adenosine of Aδ and C primary-afferent glutamatergic transmission in adult rat substantia gelatinosa neurons. Neuroscience *125*, 221–231.

Li, G.D., Wo, Y., Zhong, M.F., et al. (2002). Expression of fibroblast growth factors in rat dorsal root ganglion neurons and regulation after peripheral nerve injury. Neuroreport *13*, 1903–1907.

Li, K.C., Zhang, F.X., Li, C.L., et al. (2011). Follistatin-like 1 suppresses sensory afferent transmission by activating Na^+,K^+-ATPase. Neuron *69*, 974–987.

Lin, Y.T., Ro, L.S., Wang, H.L., et al. (2011). Up-regulation of dorsal root ganglia BDNF and trkB receptor in inflammatory pain: an in vivo and in vitro study. J. Neuroinflammation *8*, 126.

Liu, X.J., Zhang, F.X., Liu, H., et al. (2012). Activin C expressed in nociceptive afferent neurons is required for suppressing inflammatory pain. Brain *135*, 391–403.

Luo, C., Kumamoto, E., Furue, H., et al. (2002). Nociceptin inhibits excitatory but not inhibitory transmission to substantia gelatinosa neurones of adult rat spinal cord. Neuroscience *109*, 349–358.

Ma, G.Q., Wang, B., Wang, H.B., et al. (2008). Short elements with charged amino acids form clusters to sort protachykinin into large dense-core vesicles. Traffic *9*, 2165–2179.

Madiai, F., Goettl, V.M., Hussain, S.R., et al. (2005). Anti-fibroblast growth factor-2 antibodies attenuate mechanical allodynia in a rat model of neuropathic pain. J. Mol. Neurosci. *27*, 315–324.

Miki, T., Bottaro, D.P., Fleming, T.P., et al. (1992). Determination of ligand-binding specificity by alternative splicing: two distinct growth factor receptors encoded by a single gene. Proc. Natl Acad. Sci. USA *89*, 246–250.

Nakatsuka, T., Park, J.S., Kumamoto, E., et al. (1999). Plastic changes in sensory inputs to rat substantia gelatinosa neurons following peripheral inflammation. Pain *82*, 39–47.

Perkins, J.R., Antunes-Martins, A., Calvo, M., et al. (2014). A comparison of RNA-seq and exon arrays for whole genome transcription profiling of the L5 spinal nerve transection model of neuropathic pain in the rat. Mol. Pain *10*, 7–0.

Ron, D., Bottaro, D.P., Finch, P.W., et al. (1993). Expression of biologically active recombinant keratinocyte growth factor. Structure/function analysis of amino-terminal truncation mutants. J. Biol. Chem. *268*, 2984–2988.

Rubin, J.S., Osada, H., Finch, P.W., et al. (1989). Purification and characterization of a newly identified growth factor specific for epithelial cells. Proc. Natl Acad. Sci. USA *86*, 802–806.

Salio, C., Lossi, L., Ferrini, F., et al. (2005). Ultrastructural evidence for a pre- and postsynaptic localization of full-length trkB receptors in substantia gelatinosa (lamina II) of rat and mouse spinal cord. Eur. J. Neurosci. *22*, 1951–1966.

Spielberger, R., Stiff, P., Bensinger, W., et al. (2004). Palifermin for oral mucositis after intensive therapy for hematologic cancers. N. Engl. J. Med. *351*, 2590–2598.

Terauchi, A., Johnson-Venkatesh, E.M., Toth, A.B., et al. (2010). Distinct FGFs promote differentiation of excitatory and inhibitory synapses. Nature *465*, 783–787.

Umemori, H., Linhoff, M.W., Ornitz, D.M., et al. (2004). FGF22 and its close relatives are presynaptic organizing molecules in the mammalian brain. Cell *118*, 257–270.

Wang, H.B., Zhao, B., Zhong, Y.Q., et al. (2010). Coexpression of δ- and μ-opioid receptors in nociceptive sensory neurons. Proc. Natl Acad. Sci. USA *107*, 13117–13122.

Wilcox, J.N. (1993). Fundamental principles of in situ hybridization. J. Histochem. Cytochem. *41*, 1725–1733.

Xiao, H.S., Huang, Q.H., Zhang, F.X., et al. (2002). Identification of gene expression profile of dorsal root ganglion in the rat peripheral axotomy model of neuropathic pain. Proc. Natl Acad. Sci. USA *99*, 8360–8365.

Yamanaka, H., Obata, K., Kobayashi, K., et al. (2007). Activation of fibroblast growth factor receptor by axotomy, through downstream p38 in dorsal root ganglion, contributes to neuropathic pain. Neuroscience *150*, 202–211.

Yoshimura, M., and Nishi, S. (1993). Blind patch-clamp recordings from substantia gelatinosa neurons in adult rat spinal cord slices: pharmacological properties of synaptic currents. Neuroscience *53*, 519–526.

Zhang, X., Bao, L., Arvidsson, U., et al. (1998). Localization and regulation of the δ-opioid receptor in dorsal root ganglia and spinal cord of the rat and monkey: evidence for association with the membrane of large dense-core vesicles. Neuroscience *82*, 1225–1242.

Zhang, X., Bao, L., and Ma, G.Q. (2010). Sorting of neuropeptides and neuropeptide receptors into secretory pathways. Prog. Neurobiol. *90*, 276–283.

Zhang, X., Bao, L., Yang, L., et al. (2012). Roles of intracellular fibroblast growth factors in neural development and functions. Sci. China Life Sci. *55*, 1038–1044.

Zhang, X., Bao, L., and Li, S. (2015). Opioid receptor trafficking and interaction in nociceptors. Br. J. Pharmacol. *172*, 364–374.

Zhao, B., Wang, H.B., Lu, Y.J., et al. (2011). Transport of receptors, receptor signaling complexes and ion channels via neuropeptide-secretory vesicles. Cell Res. *21*, 741–753.